ISSN 1063-7710, Acoustical Physics, 2020, Vol. 66, No. 3, pp. 242–249. © Pleiades Publishing, Ltd., 2020.

NONLINEAR ACOUSTICS

Parametric Study of Driver and Reflector of Single Axis Acoustic Levitator using Finite Element Method

Saurabh Yadav[a], * and Arpan Gupta[a]

[a]*Acoustic and Vibration Laboratory, School of Engineering, Indian Institute of Technology Mandi, Himachal Pradesh, 175005 India*

**e-mail: saurabh16yadav@gmail.com*

Received November 1, 2018; revised November 11, 2019; accepted December 24, 2019

Abstract—Total radiation force on a spherical levitating object, which is placed between a single axis acoustic levitator, is obtained using finite element simulation. Variation in the total radiation force on the spherical levitating object with respect to the position of the object between the driver and the reflector is studied in resonance as well as non-resonance condition. Simulation results are verified with experimental results available in the literature. Further, a parametric study has been performed on the radius of curvature of driver and reflector. Three different cases have been considered. (1) Curved driver surface with flat reflector surface. (2) Curved reflector surface with flat driver surface. (3) Both driver and reflector having curved surfaces. It is observed that the case with both driver and reflector surfaces being curved results in maximum radiation force on the spherical levitating object. The values of radius of curvature for maximum radiation force for all three cases are also obtained. Total radiation forces for all three cases (with optimum value of radius of curvature) as well as the flat surfaced driver-reflector arrangement are compared.

Keywords: acoustic levitation, radiation force, single axis acoustic levitator, standing wave, finite element method

DOI: 10.1134/S1063771020030094

INTRODUCTION

Levitation is a process in which an upward force counteracts downward gravitational force of an object so that there is no physical contact between levitated object and ground. The object levitates freely in air or any other medium. When the sound waves are used to levitate the object, it is called as Acoustic levitation. The sound wave range of human hearing can affect the human ears. Therefore, for performing the experiments, the anechoic chamber [1] is required. Usually, the sound waves used for acoustic levitation are of ultrasonic range. There are many such materials like cesium, titanium etc., which become highly reactive when kept at elevated temperatures or in the molten state. If conventional techniques are used to handle such materials then it can affect the properties of these materials due to the contamination. To avoid such problems, acoustic levitation can be used to handle such reactive materials. Acoustic levitation can be broadly classified as near field acoustic levitation and single axis acoustic levitation. In near field acoustic levitation, the flat surfaced levitating objects can be levitated. Different studies have been performed for stability [2] of the flat levitating object during levitation as well as the transportation using pressure [3] due to the flexural vibration of the driving plate. This study focuses on the single axis acoustic levitation. Oran et al. have calculated the radiation force on different shape of objects when placed between the driver and reflector in single axis acoustic levitation system and the behavior of the liquid drop is also studied [4]. Other than levitating the different samples, acoustic levitation technique has also been used to calculate the speed of sound, density and other properties of different materials in liquid state at normal temperature as well supercooled condition [5–9]. An acoustic levitation apparatus for sub millimeter samples is successfully developed and demonstrated by levitating the solid and liquid samples up to the specific gravity of 19.3 [10]. Acoustic levitation using a high-power magneto strictive ferrite transducer of frequency 18 kHz has been studied. Solid as well as liquid samples of spherical shape with different size and weight have been levitated successfully [11]. A single axis acoustic levitator has been used to study the melting and solidification of commercial grade succinonitrile at the state when the sample is levitating in the air [12]. To calculate the required sound pressure level for acoustic levitation in single axis acoustic levitator, an equation has also been derived and verified with the experimental data [13]. Different methods have been developed or proposed for transporting the levitated particles of different sizes and materials along the axis of the standing wave acoustic levitation in water medium

[14] as well as in space where there is no medium [15]. Relation between the radiation force obtained in single axis acoustic levitation and the geometry of the driver-reflector is studied using a two-cylinder model incorporating the boundary element method. Resonance modes are also predicted successfully [16, 17]. Single axis acoustic levitation method has been used to successfully levitate samples of solid and liquid materials having highest density on the earth [18] as well as the some small living animals such as ant, ladybug and young fish [19].

Different parameters of the single axis acoustic levitator play an important role in maximizing the radiation force. Different parametric studies have been conducted to enhance the capability of the single axis acoustic levitation system [4, 16, 17]. Another important aspect of single axis acoustic levitation system is resonance condition. Single axis acoustic levitation system uses the standing waves phenomenon to levitate the particles. Standing waves are created when the levitation system meets the resonance condition. Different methods have been used to study the resonance conditions of the single axis acoustic levitation for a closed chamber [20, 21]. Boundary element method has been used to study the resonance conditions of open single axis acoustic levitation system [22]. The nonlinear behavior of the single axis acoustic levitator [23] as well as the oscillations of the solid spherical particle between the driver and the reflector [24] have been studied. Andrade et al. [25] have presented a review on the recent progresses in the field of acoustic levitation. As discussed in many publications, instead of using the flat surfaced driver and reflector, the curved surfaced driver and reflector give better radiation force for acoustic levitation. However, to date, the detailed study on the effect of radius of curvature of driver and reflector surface on levitation force has not been performed.

This paper presents the finite element study of variation of radiation force on a spherical levitating object placed between the driver and the reflector in the single axis acoustic levitation. To validate the finite element model, the finite element results are compared with the experimental results available in [4]. Further, the effect of the curved surfaced driver and reflector on the total radiation force is studied using three different cases and the comparison of the radiation force with different cases is shown.

NUMERICAL MODELING

Geometry of Single Axis Acoustic Levitator

For the finite element study of the single axis acoustic levitator, 2D axis symmetric model of COMSOL Multiphysics is used because of the symmetry of the geometry. Single axis acoustic levitation system consists of a driver and a reflector. Geometry of the simple acoustic levitation system is shown in Fig. 1a. The diameter of the driver and the reflector is taken as 35 mm and thickness is taken as 10 mm. The driver is considered as a cylindrical object which vibrates like a piston and generates the pressure waves. The reflector is also a cylindrical object which is only used to reflect the pressure waves. Both, the driver and the reflector, are considered as rigid. The thickness (10 mm) is provided to the driver and reflector so that these can be easily visualized in the complete geometry (with the air domain). It also helps in visualizing the driver and the reflector when their surfaces are provided with the radius of curvature. The diameter of 35 mm is selected so that the numerical results can be compared with the experimental results available in [4]. Also in paper [4] experiments are performed with the driver and reflector having diameter of 35 mm. The material of the driver and the reflector plates is taken as aluminum. The air gap between the driver and the reflector is 50 mm. There is a spherical levitating object of 4 mm diameter between the driver and the reflector. These specific dimensions are selected so that the finite element results can be validated with the experimental data available in [4] with same parameters.

Further, to study the effect of curved surfaces instead of flat surfaces of driver and the reflector, three different cases have been considered. A different geometry has been used for each case: (1) The surface of the reflector kept flat and the driver surface is considered as curved surface as shown in Fig. 1b. (2) The surface of the driver kept flat and the reflector surface is considered as curved surface as shown in Fig. 1c. (3) Both, driver as well as reflector, surfaces are considered as curved surfaces as shown in Fig. 1d. For each case, the radius of curvature is varied to find out the optimum value of the radius of curvature for which the total radiation force is maximum.

Procedure

Initially, the driver and the reflector are assumed as flat surfaced. The lower plate of the single axis acoustic levitator is considered as a sound source or driver and the upper plate as reflector. As discussed in [4], for the resonance condition, the distance (air gap) between the driver and the reflector is kept as 50 mm. The resonance frequency, which is around 15 kHz for 50 mm air gap, is obtained. So, for generating the sound waves, the driver is excited harmonically at resonance frequency with the normal velocity amplitude of 1.1 m/s. At 20°C and 1 atm pressure, the values of different parameters of the air medium are taken as: speed of sound—343.15 m/s, density—1.2015 kg/m^3 and the absorption coefficient—0.330804 dB/m.

For a simple rectangular geometry, the pressure wave generated by a driver can be represented by the following linear wave equation [26]

$$\nabla^2 p = \frac{1}{c_0^2}\frac{\partial^2 p}{\partial t^2}. \quad (1)$$

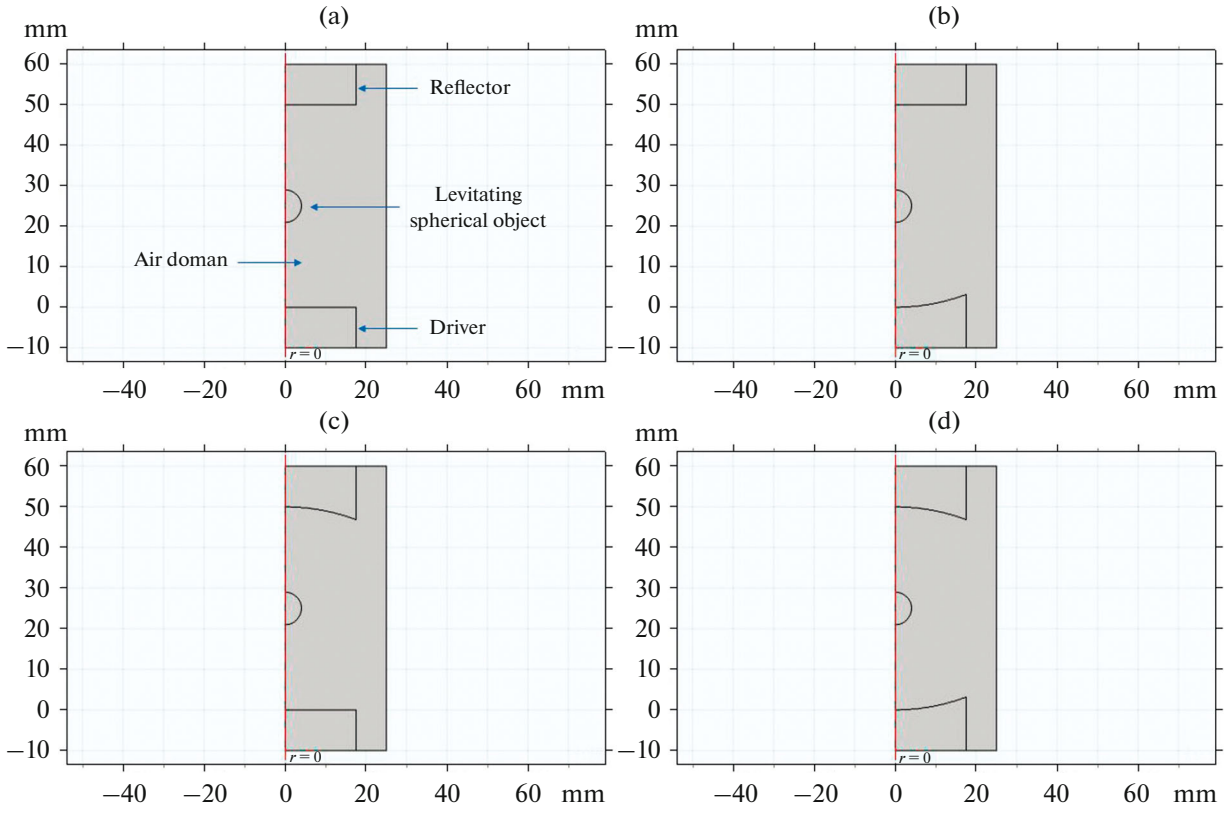

Fig. 1. Geometry of the acoustic levitator (a) with flat driver-reflector surfaces, (b) having curved driver surface with flat reflector surface (case 1), (c) having curved reflector surface with flat driver surface (case 2), (d) having both, driver as well as reflector, as curved surfaces (case 3).

In this equation, c_0 represents the speed of sound in the medium and p is the first order acoustic pressure perturbation. When the distance between the driver and the reflector is right and the sound waves emitted by the driver get reflected back from the reflector, the standing wave is formed due to the resonance. In an acoustic standing wave, the first order acoustic pressure p can be represented by [26]

$$p = p_0 \cos(\omega t)\cos(kz), \tag{2}$$

where p_0 is the pressure amplitude and $k = \omega/c_0$.

In this study, the pressure wave is generated from a piston like cylindrical driver of diameter 35 mm. A levitating object is also located between the driver and the reflector. Hence the wave existing in the domain is not a plane wave. Levitating object is considered an aluminum spherical object (bead). Oran et al. [4] have considered difference in weight on glass bead (fixed) when/not subjected to acoustic radiation force in air. Due to lack of material property, we have considered material to be aluminum (of same geometry). With respect to air both glass and aluminum are rigid ($Z_{\text{Al}} = 17.10 \times 10^5$ g/(cm^2 s), $Z_{\text{glass}} = 14.5 \times 10^5$ g/(cm^2 s), $Z_{\text{air}} = 42.9$ g/(cm^2 s)) for sound waves. Therefore, it is justifiable to use same geometry of fixed bead for finding radiation force. With these considerations, the resonance condition, i.e. the resonance frequency for the air gap of 50 mm is calculated using finite element approach. This calculated frequency is used as the excitation frequency in this study.

Further, for non-resonance condition, the excitation frequency remains same but the distance between driver and reflector is varied from 50 to 52 mm. The side boundaries of the acoustic levitator are considered as open. So, the plane wave radiation condition is assumed at the boundaries of the air domain so that there is no reflecting wave coming back from the boundaries. The following mathematical expression, which is derived from Givoli and Neta [27], represents the plane wave radiation condition in COMSOL Multiphysics.

$$-\mathbf{n}\left(-\frac{1}{\rho_c}(\nabla p_t - \mathbf{q})\right) + i\frac{k}{\rho_c}p + \frac{i}{2k\rho_c}\Delta_T p = \mathbf{n}\frac{1}{\rho_c}\nabla p_i + i\frac{k}{\rho_c}p_i + \frac{i}{2k\rho_c}\Delta_T p_i, \tag{3}$$

where $p_t = p + p_0$, p_0 is the atmospheric pressure, p is the acoustic radiation pressure, k is the wave number, ρ_c is the density of the medium, $\mathbf{q}$ is the dipole source,

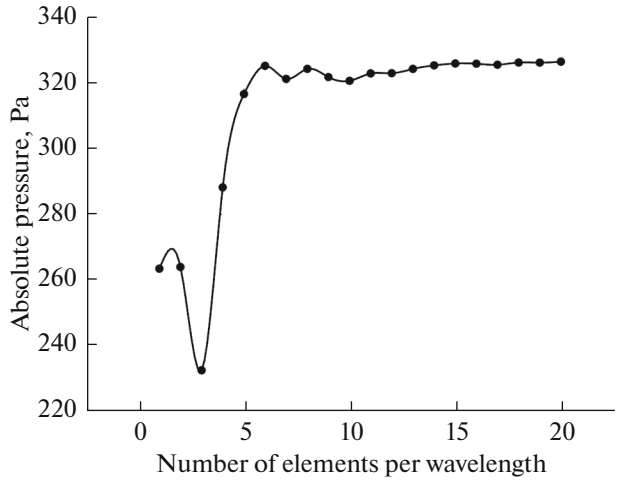

Fig. 2. Convergence plot.

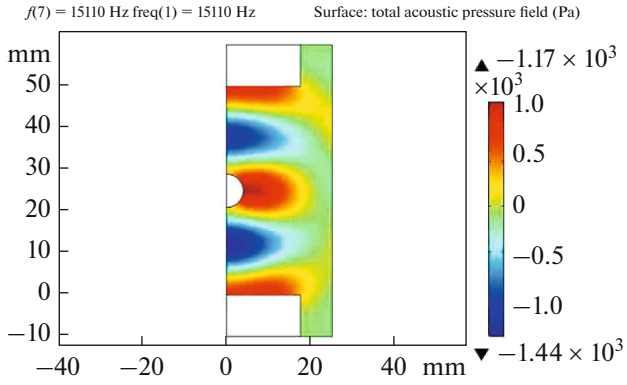

Fig. 3. Resonance condition when air gap is 2.2026 λ (50 mm).

Δ_T at a given point on the boundary denotes the Laplace operator in the tangent plane at that particular point and p_i is an optional incoming pressure field. Eq. (3) represents the general expression for the plane wave radiation condition, but in our case (this study), there is no dipole source **q** as well as no incoming pressure field p_i.

Now, the total radiation force applied to the spherical levitating object is calculated at the different positions of the spherical object. Perturbation FEA method, discussed by Glynne-Jones et al. [28], is used to calculate the radiation force on a spherical levitating object. As the position of the spherical object between the driver and the reflector varies, the value of the radiation force applied to the object also varies. So, the variation of the total radiation force with the position of the object is plotted for both conditions: one is resonance condition and the other is non-resonance condition. To validate our finite element model, these finite element results are compared with the experimental results available in [4] and both results show a good agreement. Using the same approach, the effect of varying the radius of curvature of the reflector and driver surfaces on the total radiation force is also simulated.

Finite Element Method and Convergence Study

2D six nodded free triangular elements are selected to mesh the geometry. The size of the 2D axis symmetric geometry is 25 mm in radius and 70 mm in height. The driver is situated at the bottom of the geometry and the reflector is at the top. The sides of the geometry are considered as open so the plane wave radiation condition is considered at the sides (as discussed earlier). The element size for the meshing is selected by convergence study. For convergence study, the absolute pressure at the center of the geometry (considering there is not levitating object present) is calculated and plotted with respect to the element size. As shown in Fig. 2, the solution is almost close to converged solution with element size λ/8, where λ is the wavelength. Further reducing the element size will lead to the higher computational cost. So, the element size λ/8 is selected for the simulation to get satisfactory results without increasing the unnecessary computational cost.

RESULTS AND DISCUSSION

As mentioned in [4], when the air gap between the driver and the reflector is 50 mm, the acoustic levitator is supposed to be in resonance condition with excitation frequency around 15000 Hz. Finite element simulation is used to estimate the excitation frequency for resonance condition assuming the levitating object at the center of the single axis acoustic levitator. The surfaces of driver and reflector are kept flat as shown in Fig. 3. The value of excitation frequency for resonance comes out to be 15110 Hz. Once the excitation frequency is obtained, the different parameters of acoustic levitator can be represented in the terms of a single parameter, which is the wavelength λ. The diameter of the driver and the reflector can be represented as 1.5418 λ (35 mm), the thickness of driver and reflector as 0.4405 λ (10 mm), the air gap between the driver and reflector as 2.2026 λ (50 mm) and the diameter of the spherical levitating object as 0.1762 λ (4 mm).

Now, the driver is excited harmonically with the normal velocity amplitude of 1.1 m/s at frequency of 15110 Hz. These inputs remain same for both resonance as well as non-resonance conditions. The total radiation force applied to the spherical object is calculated for both conditions. The total radiation force is plotted with respect to the position of the levitating object between the driver and the reflector. To validate the finite element model, finite element results are compared with the experimental data available in [4]. Oran et al. [4] have measured the total radiation force on a spherical object experimentally. In this experiment, a small bead was suspended along the axis of the acoustic levitation system using a thin wire passing

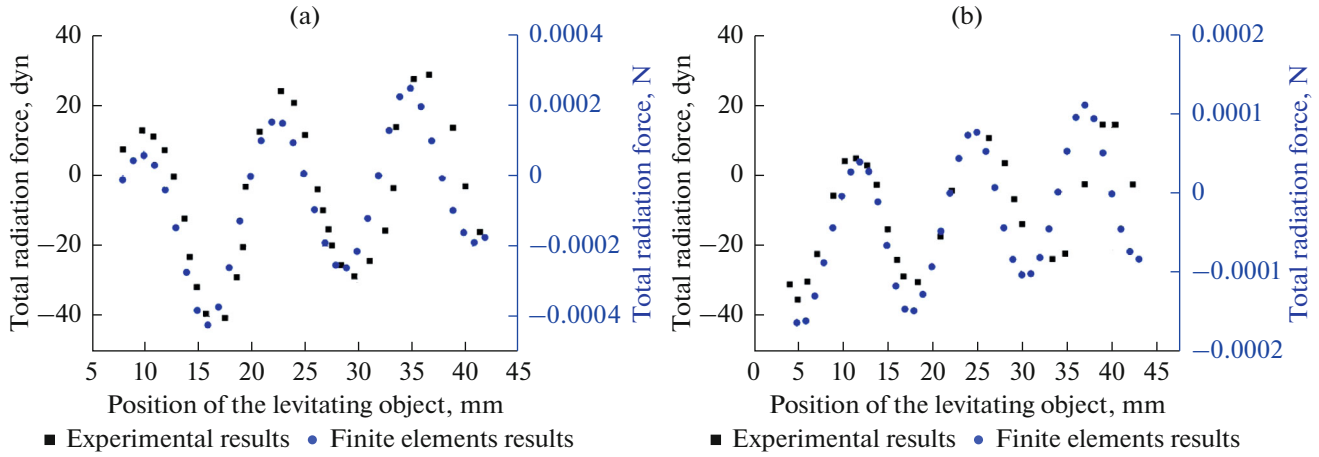

Fig. 4. Total radiation force vs position of levitating object at (a) resonance condition, (b) non-resonance condition.

through a small hole in the reflector. Other end of thin wire was connected to the arm of a Cahn balance which works on the null-balance principle. Thus, the radiation force applied to the bead was measured at the desired points for resonance as well as non-resonance condition. Finite element results are in good agreement with the experimental results of [4] for both resonance and non-resonance conditions as shown in Figs. 4a, 4b respectively.

From Fig. 4a it is also observed that the value of the total radiation force is maximum when the center of the levitating object is located at 0.7048 λ (16 mm) distance from the driver surface. For case 1, while keeping the reflector surface flat, the effect of varying the radius of curvature (Rc) of the driver on the radiation force is studied. Plot of radiation force vs Rc, with respect to the position of the levitating object, is shown in Fig. 5a. From Fig. 5a it is difficult to observe the value of radius of curvature for which the total radiation force is maximum. So, for better understanding of optimum value of radius of curvature, the levitating object is assumed to be fixed at 0.7048 λ (16 mm) distance from the driver surface. The variation of radiation force with respect to the variation of radius of curvature of the driver surface is studied as shown in Fig. 5b. It is observed that, as the radius of curvature increases, the radiation force on the levitating object also increases but after reaching the optimum value, radiation force decreases with increase in radius of curvature. The optimum value of the radius of curvature for maximum radiation force is 2.2026 λ (50 mm) for case 1. From Fig. 5a it is also observed that, by changing the radius of curvature of driver surface, the total radiation pressure on levitating object can be improved significantly at the pressure antinodes near the driver surface. As the position of levitating object shifts towards the reflector, the variation in the total radiation force is very small.

For case 2, surface of the driver is kept flat and the reflector surface is used as curved surface. Effect of varying the radius of curvature (Rc) of reflector on the total radiation force with respect to the position of the levitating object is shown in Fig. 6a. For better understanding of optimum value of radius of curvature, similar approach is used as in case 1. While keeping the levitating object at position of maximum radiation force, effect of varying radius of curvature on total radiation force is shown in Fig. 6b. The optimum value of the radius of curvature comes out to be 2.4228 λ (55 mm) for case 2. Figure 6a also shows that, by changing the radius of curvature of reflector surface, the total radiation pressure on levitating object can be improved significantly at the pressure antinodes near the reflector surface. Towards the driver end, the effect of varying the radius of curvature of reflector is very small.

For case 3, the effect of varying the radius of curvature of both (driver as well as reflector surface) on the radiation force for the different positions of the levitating object is shown in Fig. 7a. Similar to the case 1 and 2, for better understanding, the levitating object is kept at the position of maximum radiation force. The variation of radiation force with respect to the varying radius of curvature of the reflector as well as the driver surface is studied as shown in Fig. 7b. For this case, the optimum value of the radius of curvature for maximum radiation force comes as 3.7444 λ (85 mm). It is also observed from Fig. 7a that using the both (driver as well as reflector) surfaces as curved surfaces, the total radiation force is improved significantly at all the pressure antinodes.

It is observed from the results that the value of total radiation force on spherical levitating object in all three cases increases when the driver and reflector are used with curved surfaces instead of flat surfaces. It is because the curved surface tries to concentrate the sound waves towards the center axis of the single axis acoustic levitator. It can be understood clearly with the

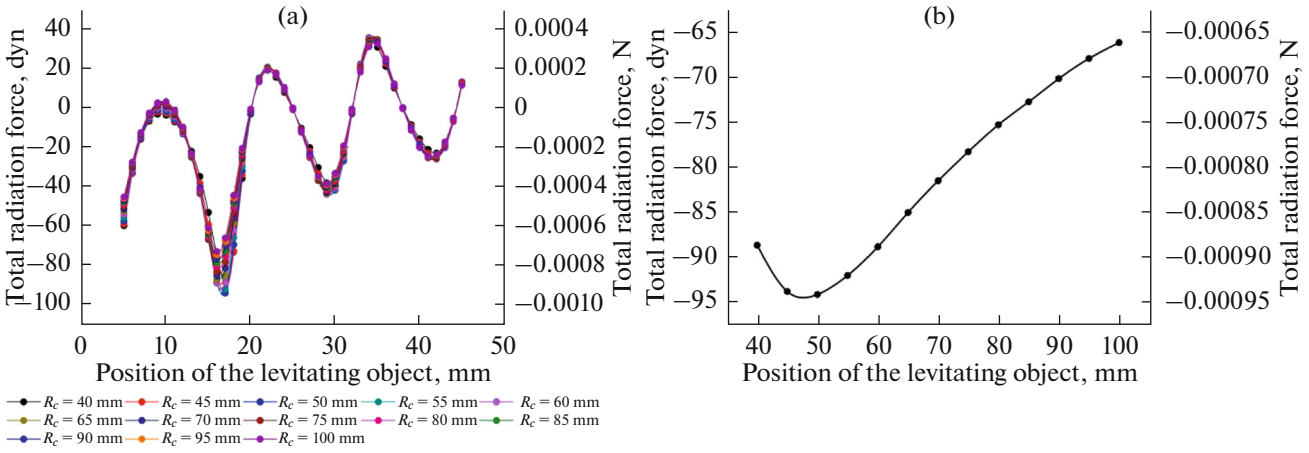

Fig. 5. (a) Total radiation force vs position of levitating object with various radius of curvature of driver, (b) total radiation force vs radius of curvature of driver.

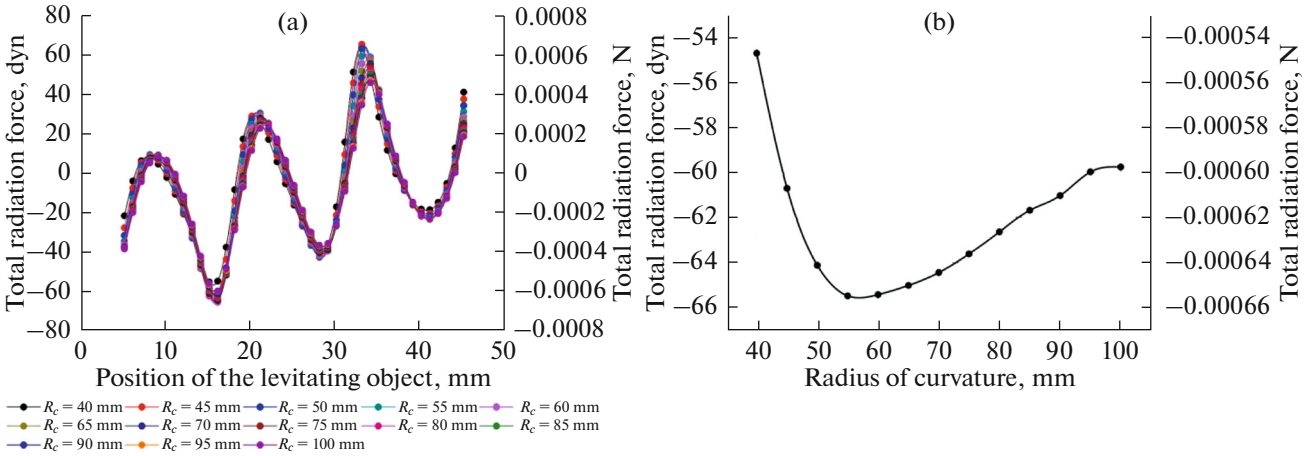

Fig. 6. (a) Total radiation force vs position of levitating object with various radius of curvature of reflector, (b) total radiation force vs radius of curvature of reflector surface.

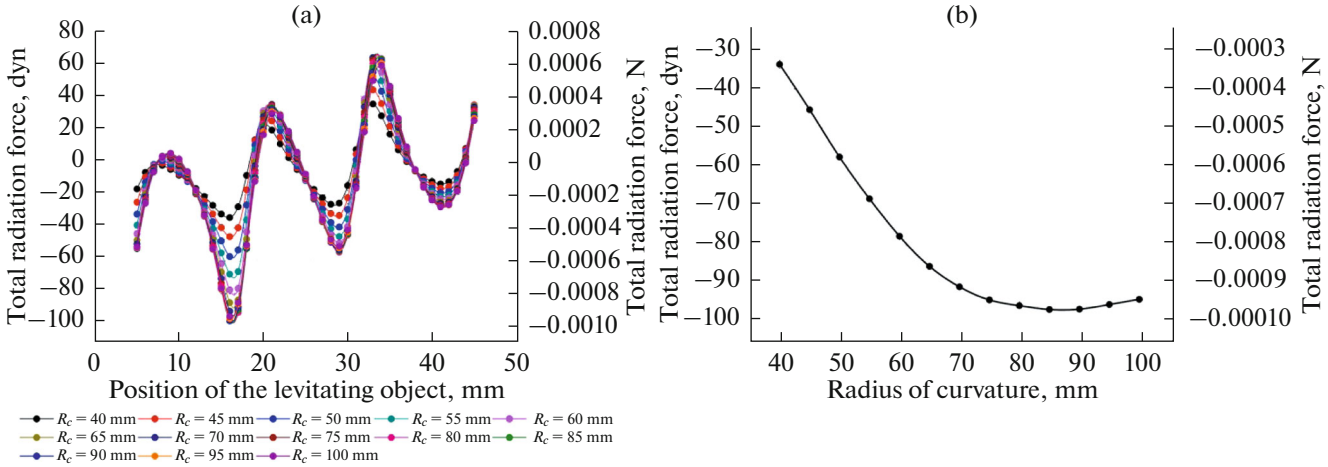

Fig. 7. (a) Total radiation force vs position of levitating object with various radius of curvature of both (driver and reflector) surfaces, (b) radiation force vs radius of curvature of both (driver and reflector) surfaces.

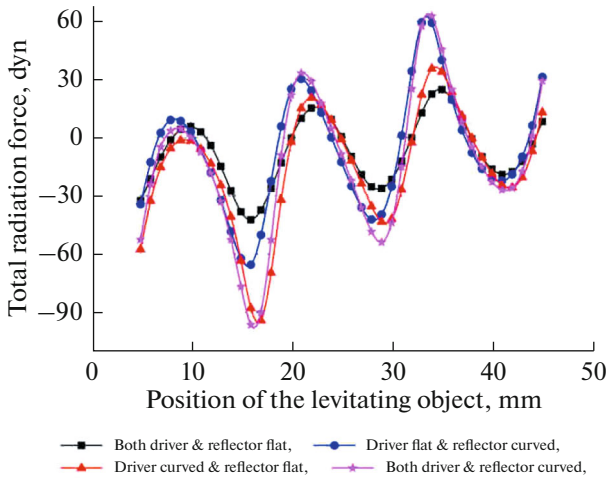

Fig. 8. Comparison of total radiation force with respect to the position of levitating object for different cases.

help of case 1. As discussed earlier, for case 1, the curved driver surface is used with flat reflector surface and the optimum value of the radius of curvature of the driver comes out to be 2.2026 λ (50 mm). It shows that the center of curvature of driver surface is at the center of the reflector surface because the air gap between the driver and the reflector or distance of reflector surface from the driver surface is also 2.2026 λ (50 mm). So, the sound waves emitted from the driver get concentrated along the axis of the acoustic levitator and high radiation force is obtained along the axis of the acoustic levitator.

Further, the total radiation pressure on levitating object is plotted for the optimal conditions of driver and reflector along with flat driver and reflector. In Fig. 8 the driver is at $x = 5$ mm end while the reflector is at $x = 45$ mm end. The optimal condition as obtained before for the radius of curvature for driver is Rc = 2.2026 λ, for reflector Rc = 2.2026 λ, and for both driver and reflector being curved, Rc = 3.7444 λ. The comparison of total radiation force with respect to the position of levitating object between driver and reflector for these four cases are shown in Fig. 8. It can be seen that the curvature (of driver or reflector) affects the corresponding nearest pressure antinode. However, curvature in either or both driver and reflector substantially increases the radiation pressure at pressure antinodes compared to flat driver and reflector.

CONCLUSION

In this paper, finite element approach is used to simulate the single axis acoustic levitator. Resonance frequency for the used geometry, shown in Fig. 1a, is obtained using finite element simulation. Variation of total radiation force with respect to the position of the levitating object is simulated and validated with the experimental data available in [4] for resonance as well as non-resonance condition. Effect of using the curved surfaces of driver and the reflector over the flat surfaces is also studied with three different cases. Optimum values of radius of curvature for case 1 (with curved driver), case 2 (with curved reflector) and case 3 (with curved driver and reflector) are obtained as 2.2026 λ (50 mm), 2.4228 λ (55 mm) and 3.7444 λ (85 mm) respectively. It is also observed that the maximum value of total radiation force on levitating object in case 3 is approximately 2.25 times the value of total radiation force with flat surfaced driver-reflector arrangement in resonance condition and approximately 6 times the value of total radiation force with flat driver-reflector surfaces in non-resonance condition. The comparative study of total radiation force with respect to the position of levitating object for optimal radius of curvatures of driver and reflector along with flat driver and reflector has been performed. The computational study can further help in designing better experiments, high radiation force and more insights in the area of acoustic levitation.

FUNDING

The authors would like to acknowledge the funding provided by SERB (Science and Engineering Research Board) through the project YSS/2015/001245.

REFERENCES

1. V. F. Kopiev, V. V. Palchikovskiy, I. V. Belyaev, Yu. V. Bersenev, S. Yu. Makashov, I. V. Khramtsov, I. A. Korin, E. V. Sorokin, and O. Yu. Kustov, Acoust. Phys. **63**, 113 (2017).
2. J. Li, C. J. Liu, and W. J. Zhang, Acoust. Phys. **63**, 125 (2017).
3. M. A. Ilgamov, Acoust. Phys. **64**, 605 (2018).
4. W. A. Oran, L. H. Berge, and H. W. Parker, Rev. Sci. Instrum. **51**, 626 (1980).
5. R. E. Apfel, J. Acoust. Soc. Am. **59**, 339 (1976).
6. E. H. Trinh and R. E. Apfel, J. Chem. Phys. **72**, 6731 (1980).
7. E. H. Trinh and C. J. Hsu, J. Acoust. Soc. Am. **80**, 1757 (1986).
8. E. H. Trinh and K. Ohsaka, Int. J. Thermophys. **16**, 545 (1995).
9. Y. Tian, R. G. Holt, and R. E. Apfel, Rev. Sci. Instrum. **66**, 3349 (1995).
10. M. C. Lee and I. Feng, Rev. Sci. Instrum. **53**, 854 (1982).
11. V. N. Bindal, T. K. Saksena, S. K. Jain, et al, Appl. Acoust. **17**, 125 (1984).
12. K. Ohsaka and E. H. Trinh, J. Cryst. Growth **96**, 973 (1989).
13. H. Mitome, in *Proc. 9th Symp. on Ultrasonic Electronics* (Sendai, 1988), p. 146.
14. M. A. Whitworth and W. T. Grundy, Ultrasonics **29**, 439 (1991).

15. T. Matsui, E. Ohdaira, N. Masuzawa, et al., Jpn. J. Appl. Phys. **34**, 2771 (1995).
16. W. J. Xie and B. Wei, Appl. Phys. Lett. **79**, 881 (2001).
17. W.-J. Xie and B.-B. Wei, Phys. Rev. E **66**, 026605 (2002).
18. W.-J. Xie, C. D. Cao, Y. J. Lü, et al., Phys. Rev. Lett. **89**, 104304 (2002).
19. W.-J. Xie, C. D. Cao, Y. J. Lü, et al., Appl. Phys. Lett. **89**, 214102 (2006).
20. E. Leung, C. P. Lee, N. Jacobi, et al., J. Acoust. Soc. Am. **72**, 615 (1982).
21. A. O. Santillan and V. Cutanda-Henríquez, J. Acoust. Soc. Am. **124**, 2733 (2008).
22. W. J. Xie and B.-B. Wei, Chin. Phys. Lett. **24**, 135 (2007).
23. M. A. Andrade, N. Pérez, and J. C. Adamowski, J. Acoust. Soc. Am. **136**, 1518 (2014).
24. M. A. Andrade, T. S. Ramos, F. T. A. Okina, et al, Rev. Sci. Instrum. **85**, 045125 (2014).
25. M. A. Andrade, N. Pérez, and J. C. Adamowski, Brazil. J. Phys. **48**, 190 (2018).
26. L. E. Kinsler, A. R. Frey, A. B. Coppens, et al., *Fundamentals of Acoustics,* 4th ed. (John Wiley Sons, 2000).
27. D. Givoli and B. Neta, J. Comput. Phys. **186**, 24 (2003).
28. P. Glynne-Jones, P. P. Mishra, R. J. Boltryk, et al., J. Acoust. Soc. Am. **133**, 1885 (2013).